Load deformation field approach from heterogeneous variations using SRBFs

When the considered variable of load effect is the geopotential differential or its linear combination, such as the load effect on gravity disturbance, vertical deflection, horizontal displacement or gravity gradient, these load Green's functions have serious high-degree oscillation and non-convergence troubles, and these load Green's function integrals have spectrum leakage and singularity problems, as shown in Fig 7.1.

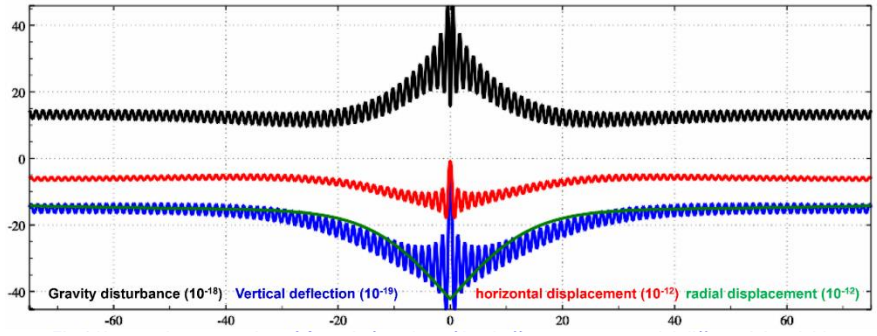

Fig 7.1 The near-zone characteristics of several load Green's functions (Indirect influence)

It is not difficult to find that when the Green's function integral is employed to calculate the load effect on the considered variable which is not dominant in the geopotential differential, such as the load effects on height anomaly, ground radial displacement or orthometric height, or load effects on ground gravity or tilt whose site has obvious vertical deformation, an acceptable integral result can be obtained. However, when being employed to calculate the load effect on gravity disturbance, vertical deflection or horizontal displacement, the integral result is very unstable, and its reliability is poor.

Similarly, for the monitoring to the land water and surface load deformation field, when the monitoring variable is GNSS ellipsoidal height variation, the regional land water variation and its load effect can be estimated by using load Green's function integral constraint. However, if the geopotential differential in the monitoring variable is dominant, such as the monitoring variable is gravity disturbance, vertical deflection, horizontal displacement or gravity gradient variations, it is difficult to obtain a stable solution by the load Green's function integral constraint method.

8.7.1 Spherical radial basis function representation of surface EWH

The surface load equivalent water height (EWH) $h_w(\boldsymbol{x})$ at the ground point $\boldsymbol{x}$ can be expressed as a linear combination of normalized surface harmonic basis functions:

$$h_w(\boldsymbol{x}) = r\sum_{n=2}^{N}\left(\frac{a}{r}\right)^n \sum_{m=-n}^{n}\bar{F}_{nm}\bar{Y}_{nm}(\boldsymbol{e}) \tag{7.1}$$

Where, $\boldsymbol{x} = r\boldsymbol{e} = r(sin\theta cos\lambda, sin\theta sin\lambda, cos\theta)$, r, λ, θ are the geocentric distance, longitude

and colatitude of the surface point $\boldsymbol{x}$ respectively, $\bar{F}_{nm}$ is the fully normalized spherical harmonic coefficient, $\bar{Y}_{nm}$ is the normalized surface harmonic basis function, and a is the equatorial radius of the Earth, which means that $\bar{Y}_{nm}$ is defined on the spherical surface with the radius of a.

$$\bar{Y}_{nm}(\boldsymbol{e}) = \bar{P}_{nm}(cos\theta)cosm\lambda, \quad \bar{F}_{nm} = \delta\bar{C}_{nm}, \quad m \geq 0$$
$$\bar{Y}_{nm}(\boldsymbol{e}) = \bar{P}_{n|m|}(cos\theta)sin|m|\lambda, \quad \bar{F}_{nm} = \bar{S}_{n|m|}, \quad m < 0 \tag{7.2}$$

Here, $\bar{P}_{nm}(cos\theta)$ is the fully normalized associative Legendre function, n is called as the degree of the harmonic coefficient, and m is called as the order of harmonic coefficient.

If the domain of the surface spherical functions are transformed from the sphere surafce with radius a to the Bjerhammar spherical surface with radius $\mathcal{R}$, then the spherical harmonic coefficients $\bar{F}_{nm}$ should be converted into $\bar{E}_{nm}$, then $h_w(\boldsymbol{x})$ can also be expressed as the linear combination in the Bjerhammar spherical surface:

$$h_w(\boldsymbol{x}) = r\sum_{n=2}^{N}\left(\frac{\mathcal{R}}{r}\right)^n\sum_{m=-n}^{n}\bar{E}_{nm}\bar{Y}_{nm}(\boldsymbol{e}) \tag{7.3}$$

On the other hand, the surface load EWH $h_w(\boldsymbol{x})$ at any surface point $\boldsymbol{x}$ can also be expressed as a linear combination of K spherical radial basis functions (SRBFs) in the Bjerhammar spherical surface:

$$h_w(\boldsymbol{x}) = a\sum_{k=1}^{K}d_k\Phi_k(\boldsymbol{x},\boldsymbol{x}_k) \tag{7.4}$$

Where, $\boldsymbol{x_k} = \mathcal{R}\boldsymbol{e_k}$ is the SRBF node defined on the Bjerhammar spherical surface, also known as the SRBF center or SRBF pole, d_k is the SRBF coefficient, K is the number of the SRBF nodes and equal to the number of SRBF coefficients, $\Phi_k(\boldsymbol{x},\boldsymbol{x_k})$ is the spherical radial basis function of the EWH can be abbreviated as $\Phi_k(\boldsymbol{x}) = \Phi_k(\boldsymbol{x},\boldsymbol{x_k})$.

The spherical radial basis function $\Phi_k(\boldsymbol{x},\boldsymbol{x_k})$ can be furtherly expanded into the Legendre series:

$$\Phi_k(\boldsymbol{x},\boldsymbol{x}_k) = \sum_{n=2}^{N}\phi_nP_n(\psi_k) = \sum_{n=2}^{N}\frac{2n+1}{4\pi}B_n\left(\frac{\mathcal{R}}{r}\right)^nP_n(\psi_k) \tag{7.5}$$

Where, ϕ_n is the degree-n Legendre coefficient of SRBF, which characterizes the shape of SRBF and determines the spatial and spectral figures of SRBF, also known as the shape factor. When the spectral domain degree-n need be not emphasized, B_n is also called as the Legendre coefficient of SRBF. $\mu = R/r$ is also called as the bandwidth parameter since it is related to the spectral domain bandwidth of the sphericalradial basis function $\Phi_k(\boldsymbol{x})$.

Substituting formula (7.5) into (7.4), we have:

$$h_w(\boldsymbol{x}) = \frac{r}{4\pi}\sum_{n=2}^{N}(2n+1)B_n\left(\frac{\mathcal{R}}{r}\right)^n\sum_{k=1}^{K}d_kP_n(\psi_k)$$
$$= \frac{r}{4\pi}\sum_{k=1}^{K}d_k\sum_{n=2}^{N}(2n+1)B_n\left(\frac{\mathcal{R}}{r}\right)^nP_n(\psi_k) \tag{7.6}$$

Considering the addition theorem of spherical harmonics:

$$P_n(\psi_k) = P_n(\boldsymbol{e}, \boldsymbol{e}_k) = \frac{4\pi}{2n+1}\sum_{m=-n}^{n} \bar{Y}_{nm}(\boldsymbol{e})\bar{Y}_{nm}(\boldsymbol{e}_k) \tag{7.7}$$

then the formula (7.5) can be written as

$$h_w(\boldsymbol{x}) = r\sum_{n=2}^{N} B_n \left(\frac{\mathcal{R}}{r}\right)^n \sum_{m=-n}^{n}\sum_{k=1}^{K} d_k \bar{Y}_{nm}(\boldsymbol{e})\bar{Y}_{nm}(\boldsymbol{e}_k) \tag{7.8}$$

Comparing formulas (7.1), (7.3) and (7.8), we have:

$$\bar{F}_{nm} = \left(\frac{\mathcal{R}}{a}\right)^n \bar{E}_{nm} = B_n \left(\frac{\mathcal{R}}{a}\right)^n \sum_{k=1}^{K} d_k \bar{Y}_{nm}(\boldsymbol{e}_k) \tag{7.9}$$

Using formula (7.9), the spherical harmonic coefficient $\bar{F}_{nm}$ can be calculated from the spherical radial basis function coefficient d_k. After that, the spherical harmonic coefficient can be employed to calculate various load effects outside the solid Earth.

The location, distribution and amount of the SRBF nodes (centers) $\{\boldsymbol{x_k}\}$ on the Bjerhammar sphere surafce are the key indicators for load deformation field approach using spherical radial basis functions, which determine the spatial degrees of freedom (spatial resolution) and spatial feature of regional load deformation field, similar to the degree of the global surface load spherical harmonic coefficient model.

8.7.2 Spherical radial basis functions suitable for load deformation field

Some spherical radial basis functions such as the point mass kernel function, Poisson kernel function, radial multipole kernel function and Poisson wavelet kernel function are all harmonic, which are suitable for load deformation field approach.

Let $\boldsymbol{x}$ be the surface calculation point and $\boldsymbol{x_k}$ be the SRBF center on the Bjerhammar spherical surface $\Omega_{\mathcal{R}}$.

(1) The point mass kernel function

The point mass kernel function is an inverse multiquadric function (IMQ) proposed by Hardy (1971), which is the kernel function of gravitational potential integral formula $V = G\iiint \frac{dm}{L}$, and can be analytically expressed as:

$$\Phi_{IMQ}(\boldsymbol{x}, \boldsymbol{x}_k) = \frac{1}{L} = \frac{1}{|\boldsymbol{x}-\boldsymbol{x}_k|} \tag{7.10}$$

Where, L is the space distance between $\boldsymbol{x}$ and $\boldsymbol{x_k}$. Since $\Delta(1/L) = 0$, the point mass kernel function $\Phi_{IMQ}(\boldsymbol{x}, \boldsymbol{x_k})$ satisfies the Laplace equation.

(2) The Poisson kernel function

The Poisson kernel function is derived from the Poisson integral formula, and can be analytically expressed as::

$$\Phi_P(\boldsymbol{x}, \boldsymbol{x}_k) = -2r\frac{\partial}{\partial r}\left(\frac{1}{L}\right) - \frac{1}{L} = \frac{r^2 - r_k^2}{L^3} \tag{7.11}$$

Here, r, r_k are the spherical radial distance (namely spherical center distance) of $\boldsymbol{x}$ and $\boldsymbol{x_k}$,

respectively.

(3) The radial multipole kernel function

The analytical expression of the radial multipole kernel function is:

$$\Phi_{RM}^{m}(\boldsymbol{x},\boldsymbol{x}_k)=\frac{1}{m!}\left(\frac{\partial}{\partial r_k}\right)^{m}\frac{1}{L} \tag{7.12}$$

Where, m can be called as the order of the radial multipole kernel function, and the zero-order radial multipole kernel function is the point mass kernel function, namely $\Phi_{IMQ}(\boldsymbol{x},\boldsymbol{x}_k)=\Phi_{RM}^{0}(\boldsymbol{x},\boldsymbol{x}_k)$.

(4) The Poisson wavelet kernel function

The analytical expression of the Poisson wavelet kernel function is:

$$\Phi_{PW}^{m}(\boldsymbol{x},\boldsymbol{x}_k)=2(\chi_{m+1}-\chi_m),\quad \chi_m=\left(r_k\frac{\partial}{\partial r_k}\right)^{m}\frac{1}{L} \tag{7.13}$$

The zero-order Poisson wavelet kernel function is the Poisson kernel function $\Phi_P(\boldsymbol{x},\boldsymbol{x}_k)=\Phi_{PW}^{0}(\boldsymbol{x},\boldsymbol{x}_k)$.

(5) Calculation of spherical radial basis functions

The spherical radial basis function analytical expressions (7.10) ~ (7.13) are usually expressed in the Legendre series (7.5), and then calculated according to the Legendre expansion to highlight the spectral domain figures of the load deformation field.

ETideLoad4.5 normalizes the Legendre expansion of the spherical radial basis function $\Phi_k(\boldsymbol{x},x_k)$, and then calculates the spherical radial basis functions (SRBF) using the normalized Legendre expansion.

Let the spherical angular distance $\psi_k=0$ from $\boldsymbol{x}_k$ to $\boldsymbol{x}$, then $cos\psi_k=1$, $P_n(cos\psi_k)=P_n(1)=1$, substitute these into formula (7.5), we have the general expression of the normalization coefficient of SRBF:

$$\Phi^0=\sum_{n=2}^{N}\frac{2n+1}{4\pi}B_n\mu^n \tag{7.14}$$

The Legendre expansion of the normalized spherical radial basis function is:

$$\Phi_k(\boldsymbol{x},\boldsymbol{x}_k)=\frac{1}{\Phi^0}\sum_{n=2}^{N}\phi_nP_n(\psi_k)=\frac{1}{\Phi^0}\sum_{n=2}^{N}\frac{2n+1}{4\pi}B_n\mu^nP_n(\psi_k) \tag{7.15}$$

The mentioned four forms of SRBF and their corresponding Legendre coefficients are shown in Tab 7.1.

Tab 7.1 Spherical radial basis functions (SRBFs) and corresponding Legendre coefficients

SRBF	$\Phi_k(x,x_k)$	ϕ_n	B_n
Point mass kernel	$\frac{1}{L}=\frac{1}{\lvert x-x_k\rvert}$	μ^n	$\frac{4\pi}{2n+1}$

Poisson kernel function	$\frac{r^2-r_k^2}{L^3}$	$(2n+1)\mu^n$	4π
radial multipole kernel	$\frac{1}{m!}\left(\frac{\partial}{\partial r_k}\right)^m \frac{1}{L}$	$C_n^m \mu^{n-m} \ \ (n \geq m)$	$\frac{4\pi C_n^m}{2n+1}\mu^{-m}$
Poisson wavelet kernel	$2(\chi_{m+1}-\chi_m)$ $\chi_m = \left(r_k \frac{\partial}{\partial r_k}\right)^m \frac{1}{L}$	$(-nln\mu)^m(2n+1)\mu^n$	$4\pi(-nln\mu)^m$

8.7.3 Unit spherical Reuter grid construction algorithm

Given the Reuter grid level Q (even number), the geocentric latitude interval $d\varphi$ of the unit spherical Reuter grid in the spherical coordinate system and the geocentric latitude φ_i of the center of the cell-grid i are respectively

$$d\varphi = \frac{\pi}{Q}, \quad \varphi_i = -\frac{\pi}{2} + \left(i - \frac{1}{2}\right)d\varphi, \quad 1 \leq i < Q \tag{7.16}$$

The cell-grid number J_i in the prime vertical circle direction at latitude φ_i, the longitude interval $d\lambda_i$ and the side length dl_i are respectively

$$J_i = \left[\frac{2\pi cos\varphi_i}{d\varphi}\right], \quad d\lambda_i = \frac{2\pi}{J_i}, \quad dl_i = d\lambda_i cos\varphi_i \tag{7.17}$$

It is not difficult to find that $dl_i \approx d\varphi$. Let

$$\varepsilon_i = \frac{ds_i - ds}{ds} = \frac{dl_i - d\varphi}{d\varphi} = \frac{d\lambda_i}{d\varphi}cos\varphi_i - 1 \tag{7.18}$$

Where, ds is the cell-grid area near the equator, ds_i is the cell-grid area at the prime vertical circle φ_i, and ε_i is the relative bias of the parallel circle cell-grid area relative to the cell-grid area near the equator.

ε_i is generally small, about a few ten-thousandth, and the value is related to the Reuter grid level Q. Near the equator, we have $ds = d\varphi \cdot d\varphi$, $\varepsilon_{Q/2} = 0$.

Given the range of longitude and latitude of the local area, you can directly determine the minimum and maximum value of i according to the formula (7.16), and then calculate the maximum J_i at each prime vertical circle according to the formula (7.17), to determine the regional Reuter grid whose level is Q without calculating the global grid.

8.7.4 SRBF representation for load effects on all-element geodetic variations

According to the surface load effect spherical harmonic series expansion (2.8)~(2.20), the spherical radial basis function parameterization of the load effects on various geodetic variations can be derived from surface EWH spherical radial basis function expansion (7.6) as follows. Where, the SRFB parameterization of surafce EWH is rewritten as:

$$\Delta h_w(\boldsymbol{x}) = r\sum_{k=1}^{K} d_k \sum_{n=2}^{N}(2n+1)B_n\left(\frac{\mathcal{R}}{r}\right)^n P_n(\psi_k) \tag{7.19}$$

SRFB parameterization of the load effect on height anomaly:

$$\Delta\zeta = \frac{3\rho_w}{\rho_e}\frac{GM}{\gamma r}\sum_{k=1}^{K} d_k \sum_{n=2}^{N} B_n(1+k'_n)\left(\frac{\mathcal{R}}{r}\right)^n P_n(\psi_k) \tag{7.20}$$

SRFB parameterization of the load effect on ground gravity◉:

$$\Delta g^s = \frac{3\rho_w}{\rho_e}\frac{GM}{r^2}\sum_{k=1}^{K} d_k \sum_{n}^{\square}(n+1)\left(1+\frac{2}{n}h'_n-\frac{n+1}{n}k'_n\right)B_n\left(\frac{\mathcal{R}}{r}\right)^{n-1} P_n(\psi_k) \tag{7.21}$$

SRFB parameterization of the load effect on gravity (distrubance):

$$\Delta g^\delta = \frac{3\rho_w}{\rho_e}\frac{GM}{r^2}\sum_{k=1}^{K} d_k \sum_{n}^{\square}(n+1)(1+k'_n)B_n\left(\frac{\mathcal{R}}{r}\right)^{n-1} P_n(\psi_k) \tag{7.22}$$

SRFB parameterization of the load effect on ground tilt◉:

$$\text{South: } \Delta\xi^s = \frac{3\rho_w}{\rho_e}\frac{GM}{\gamma r^2}\sum_{k=1}^{K} d_k\, cos\alpha_k \sum_{n}^{\square}(1+k'_n-h'_n)B_n\left(\frac{\mathcal{R}}{r}\right)^n \frac{\partial P_n(\psi_k)}{\partial\psi_k} \tag{7.23}$$

$$\text{West: } \Delta\eta^s = \frac{3\rho_w}{\rho_e}\frac{GM}{\gamma r^2}\sum_{k=1}^{K} d_k\, sin\alpha_k \sum_{n}^{\square}(1+k'_n-h'_n)B_n\left(\frac{\mathcal{R}}{r}\right)^n \frac{\partial P_n(\psi_k)}{\partial\psi_k} \tag{7.24}$$

SRFB parameterization of the load effect on vertical deflection:

$$\text{South: } \Delta\xi = \frac{3\rho_w}{\rho_e}\frac{GM}{\gamma r^2}\sum_{k=1}^{K} d_k\, cos\alpha_k \sum_{n}^{\square}(1+k'_n)B_n\left(\frac{\mathcal{R}}{r}\right)^n \frac{\partial P_n(\psi_k)}{\partial\psi_k} \tag{7.25}$$

$$\text{West: } \Delta\eta = \frac{3\rho_w}{\rho_e}\frac{GM}{\gamma r^2}\sum_{k=1}^{K} d_k\, sin\alpha_k \sum_{n}^{\square}(1+k'_n)B_n\left(\frac{\mathcal{R}}{r}\right)^n \frac{\partial P_n(\psi_k)}{\partial\psi_k} \tag{7.26}$$

SRFB parameterization of the load effect on ground site displacement ◉:

$$\text{East: } \Delta e = -\frac{3\rho_w}{\rho_e}\frac{GM}{\gamma r}\sum_{k=1}^{K} d_k\, cos\alpha_k \sum_{n}^{\square} l'_n B_n\left(\frac{\mathcal{R}}{r}\right)^n \frac{\partial P_n(\psi_k)}{\partial\psi_k} \tag{7.27}$$

$$\text{North: } \Delta n = -\frac{3\rho_w}{\rho_e}\frac{GM}{\gamma r}\sum_{k=1}^{K} d_k\, sin\alpha_k \sum_{n}^{\square} l'_n B_n\left(\frac{\mathcal{R}}{r}\right)^n \frac{\partial P_n(\psi_k)}{\partial\psi_k} \tag{7.28}$$

$$\text{Radial: } \Delta r = \frac{3\rho_w}{\rho_e}\frac{GM}{r\gamma}\sum_{k=1}^{K} d_k \sum_{n=2}^{N} B_n h'_n\left(\frac{\mathcal{R}}{r}\right)^n P_n(\psi_k) \tag{7.29}$$

SRFB parameterization of the load effect on normal (orthometric) height◉:

$$\Delta\mathcal{H} = \frac{3\rho_w}{\rho_e}\frac{GM}{\gamma r}\sum_{k=1}^{K} d_k \sum_{n=2}^{N} B_n(h'_n-k'_n-1)\left(\frac{R}{r}\right)^n P_n(\psi_k) \tag{7.30}$$

SRFB parameterization of the load effect on gravity gradient:

$$\text{Radial: } \Delta T_{rr} = \frac{3\rho_w}{\rho_e}\frac{GM}{r^3}\sum_{k=1}^{K} d_k \sum_{n}^{\square}(n+1)(n+2)(1+k'_n)B_n\left(\frac{\mathcal{R}}{r}\right)^{n-1} P_n(\psi_k) \tag{7.31}$$

$$\text{North: } \Delta T_{NN} = \frac{3\rho_w}{\rho_e}\frac{GM}{r^3}\sum_{k=1}^{K} d_k \frac{\partial^2\psi_k}{\partial\varphi_k^2}\sum_{n}^{\square}(1+k'_n)B_n\left(\frac{\mathcal{R}}{r}\right)^n \frac{\partial^2 P_n(\psi_k)}{\partial\psi_k^2} \tag{7.32}$$

$$\text{West: } \Delta T_{WW} = -\frac{3\rho_w}{\rho_e}\frac{GM}{r^3 cos^2\varphi}\sum_{k=1}^{K} d_k \frac{\partial^2\psi_k}{\partial\lambda_k^2}\sum_{n}^{\square}(1+k'_n)B_n\left(\frac{\mathcal{R}}{r}\right)^n \frac{\partial^2 P_n(\psi_k)}{\partial\psi_k^2} \tag{7.33}$$

Where, α_k is the geodetic azimuth of ψ_k.

In the mentioned expressions, the load effects on the geodetic variations marked ◉ are valid only when their sites are fixed with the solid Earth, and that on the remaining geodetic

variations are suitable on the ground or outside the solid Earth.

Similar to the spatial load Green's function integral method, if the regional surface load equivalent water height h_w is known, the SRBF spectral domain analysis of the load equivalent water height h_w can be performed according to Formula (7.19) to estimate the SRBF coefficients. ETideLoad4.5 calls this process as the load SRBF approach. The regional all-element load deformation field can be calculated from SRBF coefficients according to Formulas (7.20) to (7.33). ETideLoad4.5 calls this process as the load effect SRBF synthesis.

Here, the point mass kernel function is selected as SRBF, and the minimum and maximum degree are set to be 90 and 1800 respectively. The buried depth of the Bjerhammar sphere is set to be 5 km, and the maximum action distance of SRBF center is 150 km. The SRBF spatial curves of the load effects on gravity disturbance, vertical deflection, horizontal displacement, and radial displacement are calculated, as shown in Fig 2.

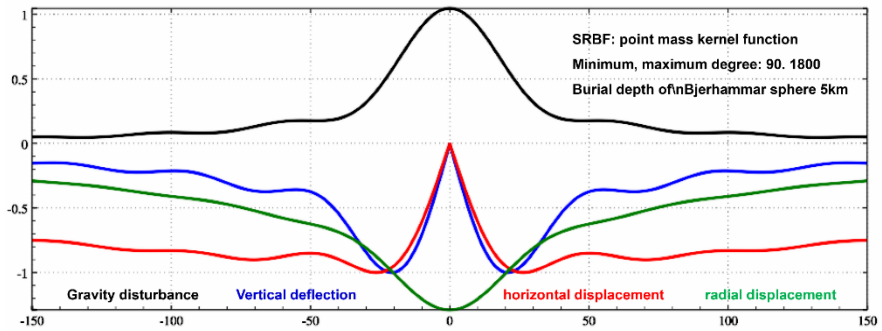

Fig 7.2 The near-zone characteristics of load effect SRBFs on several geodetic variations

Comparing Fig 7.1 and Fig 7.2, it can be seen that the convergence property of SRBF near the calculation point is obviously better than that of load Green's function even for the load effect on radial displacement. The SRBFs of load effects on gravity disturbance, vertical deflection and horizontal displacement are monotonically convergent within 20 km near the calculation point. It can be seen that the high-degree oscillation and non-convergence problems of load Green's function can be effectively solved by using SRBF instead.

8.7.5 First and second order horizontal partial derivatives of ψ

The algorithm formulas of the SRBFs of the load effect need to employ the horizontal first-order and second-order partial derivatives of the spherical angle distance ψ, whose derivation process in the spherical coordinate system is given below.

$$\frac{\partial \psi}{\partial \varphi} = -cos\alpha, \quad \frac{\partial \psi}{\partial \lambda} = -cos\varphi sin\alpha \tag{7.34}$$

Where, α is the geodetic azimuth of ψ, which can be obtained from the spherical trigonometric formulas:

$$sin\psi cos\alpha = cos\varphi sin\varphi' - sin\varphi cos\varphi' cos(\lambda' - \lambda) \tag{7.35}$$

$$sin\psi sin\alpha = cos\varphi' sin(\lambda' - \lambda) \tag{7.36}$$

Taking the partial derivative with respect to φ on both sides of Equation (7.35), considering (7.34), we have:

$$-cos\psi cos^2\alpha + sin\psi \frac{\partial^2\psi}{\partial\varphi^2} = -\sin\varphi sin\varphi' - cos\varphi cos\varphi' cos(\lambda' - \lambda) \tag{7.37}$$

so that we have:

$$sin\psi \frac{\partial^2\psi}{\partial\varphi^2} = -\sin\varphi sin\varphi' - cos\varphi cos\varphi' cos(\lambda' - \lambda) + cos\psi cos^2\alpha \tag{7.38}$$

In the same way, taking the partial derivatives of both sides of Equation (7.36) with respect to λ, we have:

$$-cos\psi cos\varphi sin^2\alpha + sin\psi \frac{\partial^2\psi}{\partial\lambda^2} = -cos\varphi' sin(\lambda' - \lambda) \tag{7.39}$$

$$sin\psi \frac{\partial^2\psi}{\partial\lambda^2} = -cos\varphi' sin(\lambda' - \lambda) + cos\psi cos\varphi sin^2\alpha \tag{7.40}$$

8.7.6 Regional SRBF approach of surface loads and synthesis of load effects

Similar to the ‘Remove - load Green's function integral - Restore’ scheme of regional load deformation field approach using the load spherical harmonic coefficient model reference field, the regional high-resolution load deformation field SRBF approach can also adopt the ‘remove- load SRBF approach-restore’ scheme based on the load spherical harmonic coefficient model reference field. Here, the residual load SRBF approach is employed to instead of the residual load Green's function integral.

(1) The scheme for SRBF approach of residual loads and synthesis of load effects

Similar to the global load spherical harmonic analysis and the load effect spherical harmonic synthesis process, the residual load SRBF approach scheme also consists of two steps. In the first step, according to the regional surface load SRBF spectral domain expansion (7.19), the SRBF coefficients $\{d_k\}$ are estimated by the least square method from the regional residual EWHs. The step can be called as the regional load SRBF analysis. In the second step, according to the regional load effect SRBF synthesis algorithm formulas (7.20) ~ (7.33), the SRBF coefficients $\{d_k\}$ are employed to calculate the residual load effects on various geodetic variations. The second step can be called as the SRBF synthesis for regional load effects.

Similar to the global load spherical harmonic analysis method, the cumulative iterative SRBF analysis scheme can be employed to improve the SRBF approach level of regional residual EWHs.

(2) SRBF approach example of regional load deformation field using remove-restore scheme

The regional SRBF approach of the high-resolution load deformation field can also adopt the remove-restore scheme, that is, the 'load Green's function integral' in the 'remove-load Green's function integral-restore' scheme is replaced by 'load SRBF approach'. Where, the 'load SRBF approach' adopts a smaller SRBF center action distance (similar to the integral radius of the Green's function) to construct the residual EWH observation equation and estimate the SRBF coefficients. Then, the high-resolution residual grid of regional load deformation field is obtained by SRBF synthesis. The scheme can be called as the ‘remove - load SRBF approach - restore’ scheme.

Taking the 1′×1′ land water equivalent water height (EWH) variation grid (cm) at a sampling epoch time on May 30, 2018 in a region of southern China (taking the mean value of land water variation in the region in 2018 as the monitoring datum) as an example, the key steps of the SRBF approach of regional load deformation field are introduced. The land water here includes only 4m shallow soil water, wetland and vegetation water, but not including lakes, rivers and groundwater. The reference load deformation field adopts the 360-degree global terrestrial water variation load spherical harmonic coefficient model constructed in section 8.2.6 on May 30, 2018.

Similar to the regional refinement scheme of load Green's integral, the land water EWH variation grid area (the calculation area) should be generally bigger than refine result area of the load deformation field to suppress the edge effect. In this case, the calculation area is 97˚~103˚E, 24˚~29˚N, and the result area is 98.5˚~101.5˚E, 25.5˚~27.5˚N.

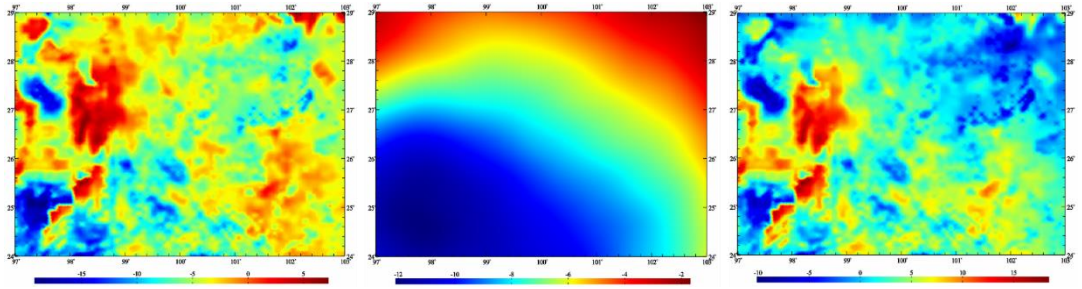

Fig 7.3 The 1′×1′ land water EWH variation obseration, model value and residual grid in the calculation area

The step 1: Input the 1′×1′ zero value grid in the calculation area (zero value means that the height of calculation point relative to the ground is equal to zero), select the maximum calculation degree of 360, and calculate the 1′×1′ land water EWH variation reference model value grid in the calculation area from the global land water load spherical harmonic coefficient model, as shown in Fig 7.3 left.

The step 2: The 1′×1′ land water EWH residual value grid (Fig 7.3 right) is generated by subtracting the 1′×1′ land water EWH observation grid (Fig 7.3 left) from the 1′×1′ land water EWH model value grid (Fig 7.3 middle).

The step 3: According to the load EWH SRBF expansion (7.19), the SRBF observation equations are constructed from the 1'×1' land water EWH variation residual grid, and the SRBF coefficients are estimated using the iterative least square method to cumulatively approach the EWH variation residual grid. Then, from the SRBF coefficients, according to load effect SRBF synthesis algorithm formulas (7.20) ~ (7.33), the 1′×1′ land water load deformation field residual grid are calculated, as shown in Fig 7.4.

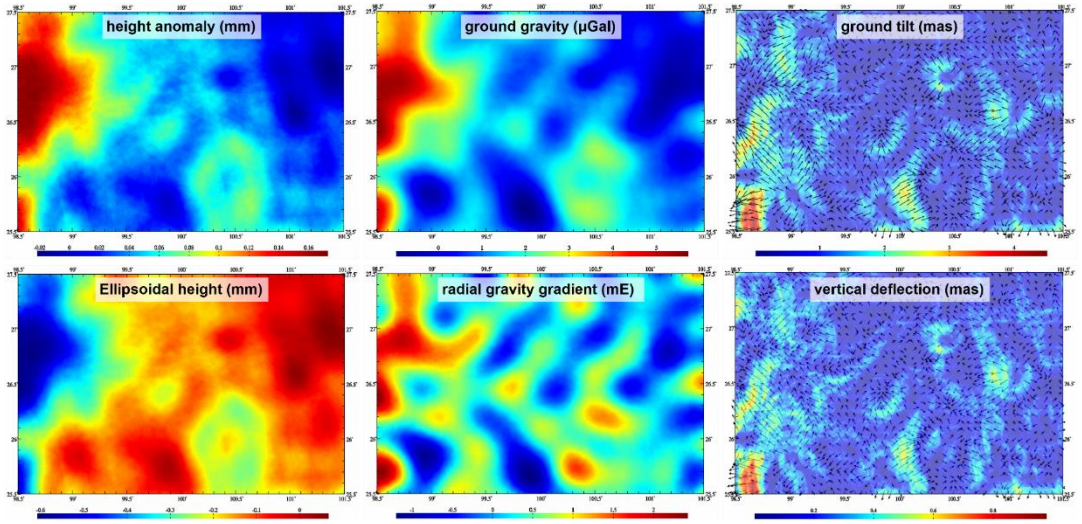

Fig 7.4 The 1′×1′ land water load deformation field residual value grid using load SRBF approach

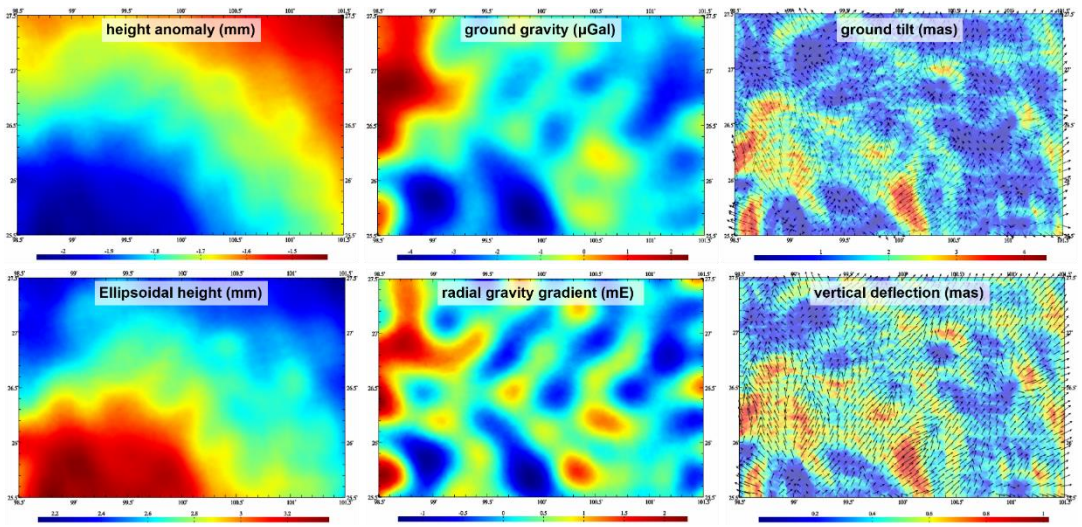

Fig 7.5 The 1′×1′ land water variation load deformation field grid refined using SRBFs in the result area

The step 4: Input the 1′×1′ zero value grid in the result area, select the maximum

calculation degree of 360, and calculate the 1′×1′ land water load deformation field model value grid from the global land water load spherical harmonic coefficient model.

The step 5: the 1′×1′ land water load deformation field residual value grid in the result area is added to the reference model value grid to obtain the 1′×1′ land water variation load deformation field grid refined in the result area, as shown in Fig 7.5.

Compared with the 8.5.5 section process, it is not difficult to find that the ‘remove - load SRBF approach - restore’ scheme and the 'remove - load Green's function integral - restore' scheme are only different in the step 3, while the step 1, 2, 4 and 5 are exactly the same.

(3) SRBF coefficients estimation with edge effect suppression

Substituting the Legendre coefficient B_n in Tab 7.1 into the load EWH SRBF expansion (7.19), we can obtain the observation equations with the residual EWH variations $\Delta\tilde{h}_w(\boldsymbol{x}_i)$ as the observations and the SRBF coefficients $\{d_k\}$ as the unknowns.

$$\boldsymbol{L} = \left\{\Delta\tilde{h}_w(\boldsymbol{x}_i)\right\}^T = \boldsymbol{A}\{d_k\}^T + \boldsymbol{\epsilon} \quad \left(i = 1,\cdots,M;\ k = 1,\cdots,K\right) \tag{7.41}$$

Where, $\boldsymbol{A}$ is the $M \times K$ design matrix, $\boldsymbol{\epsilon}$ is the $M \times 1$ observation error vector, M is the number of observations, K is the number of RBF centers, that is, the number of unknowns $\{d_k\}$, and $\boldsymbol{x}_i$ is the location coordinates of the observations.

ETideLoad proposes an algorithm that can improve the performance of parameter estimation by suppressing edge effect. When the SRBF center v is located at the margin of the calculation area, its corresponding SRBF coefficient is set to zero, that is, $d_v = 0$ as the observation equation to suppress the edge effect. The normal equation with the additional suppression of edge effect constructed by ETideLoad is:

$$[\boldsymbol{A}^T\boldsymbol{P}\boldsymbol{A} + Q\Xi]\{d_k\}^T = \boldsymbol{A}^T\boldsymbol{P}\boldsymbol{L} \tag{7.42}$$

Here, Ξ is a diagonal matrix, whose element is equal to 1 only when the SRBF center corresponding to its subscript is in the margin of the area, and the others are zero. Q is equal to the root mean square of the non-zero diagonal elements of the coefficient matrix $\boldsymbol{A}^T\boldsymbol{P}\boldsymbol{A}$ of normal equation.

The action distance dr of SRBF centers is required to be equal to maintain the spatial consistency of the approach performance of load deformation field. Where dr corresponds to the argument domain of the SRBF coefficient, so any observation is a linear combination of the SRBFs whose centers only within the radius dr.

ETideLoad improves the ill-conditioned or singularity of $\boldsymbol{A}^T\boldsymbol{P}\boldsymbol{A}$ by adding some observation equations that can suppresses edge effect to improve the stability and reliability of parameter estimation.

(4) Comparative analysis of calculation results between the load Green's function integral and SRBF approach

The step 3 in the calculation process of the ‘remove - load SRBF approach - restore’

scheme above is replaced by the load Green's function integral, which becomes the 'remove - load Green's function integral - restore' process, namely,

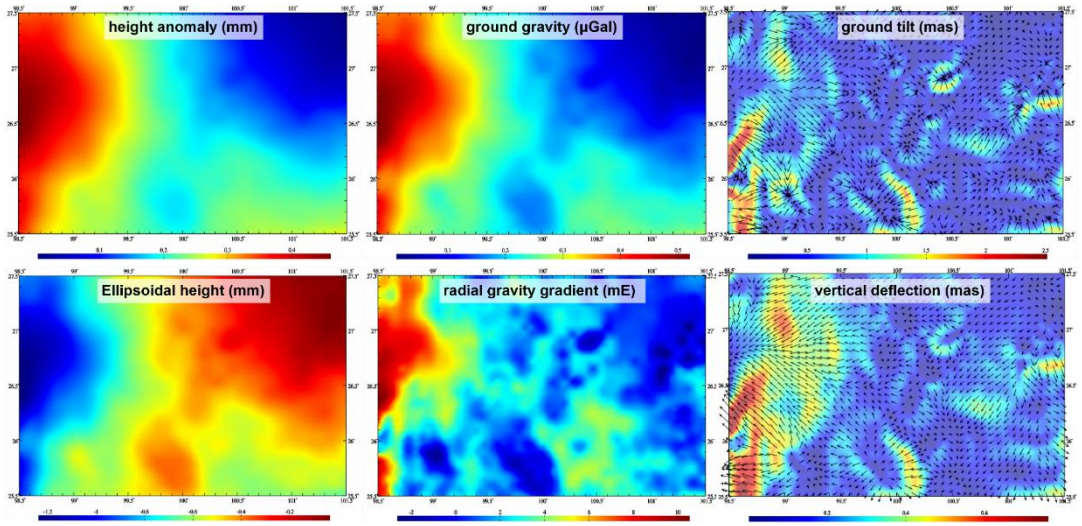

Fig 7.6 The 1′×1′ land water load deformation field residual value grid using load Green's integral

The step 3: From the 1'×1' land water EWH variation residual grid, the integral radius (equivalent to the center distance of SRBF) of 150 km selected, the 1′×1′ land water load deformation field residual grid are calculated according to load Green's function integral formulas, as shown in Fig 7.6.

Comparing Fig 7.4 and Fig 7.6, it can be seen that the spatial distribution characteristics of various geodetic variations of load effects calculated by the two schemes are all similar. The numerical results by the load Green's function integral are larger, and the spatial short-wave structure of numerical results by the load SRBF approach are rich.

8.7.7 Principle of cooperative monitoring from multiple heterogeneous geodetic techniques

ETideLoad4.5 proposes a deep fusion method for multi-source heterogeneous observation systems with good universality. Without losing generality, it is assumed that there are multiply heterogeneous geodetic monitoring techniques for a certain monitoring purpose. We can always express abstractly the monitoring purpose as a set of common parameters shared by various geodetic techniques, so as to transform the cooperative monitoring problem from multiply heterogeneous geodetic techniques into a mathematical problem on jointly solving of the common parameters.

The general scheme for solving such problems can be summarized as follows: (1) The observation equations with the common parameters as unknown parameters are composed of the monitoring variations from each group of geodetic techniques according to their

respective geodetic system structures (namely the covariance structure based on respective geodetic principle), and then these normal equations are constructed according to the principle of least squares and normalized, respectively. (2) According to the monitoring quality of each geodetic technique (system), the normal equations are weighted respectively, and the combined normal equations are generated by weighted summation to solve the unknown common parameters.

For different geodetic techniques, the types and spatial distribution of monitoring variations and covariance properties of geodetic monitoring systems are generally different. It is necessary to normalize these different groups of normal equations (covariance structures) in order to effectively control the deep fusion of various types of monitoring variations using the respective covariance structure. The combined normal equation can be expressed as:

$$\sum_s \left(\frac{w_s}{Q_s}\boldsymbol{A}_s^T\boldsymbol{P}_s\boldsymbol{A}_s\right)\boldsymbol{X} = \sum_s \left(\frac{w_s}{Q_s}\boldsymbol{A}_s^T\boldsymbol{P}_s\boldsymbol{L}_s\right) \tag{7.43}$$

Where, $s = 1, \cdots, S$, S is the number of groups; $\boldsymbol{X}$ is the common parameter vector to be estimated ; $\boldsymbol{A}_s, \boldsymbol{L}_s$ and $\boldsymbol{P}_s$ are the design matrix, observation vector and observation weight matrix of the observation equation from the s group, respectively. The $\boldsymbol{P}_s$ of the observations from the s group is only employed to distinguish the difference between the group s of observation errors, which is completely independent with other group of observation errors. Q_s is the normalized parameter of the group s of normal equation, which can be the root mean square of the non-zero diagonal elements of the group s of normal equation coefficient matrix $\boldsymbol{A}_s^T\boldsymbol{P}_s\boldsymbol{A}_s$. w_s is the group s of weight only employed to distinguish the observation quality of different groups. Because the number S of the groups is generally not large (such as $S < 10$), it is easy to furtherly optimize w_s using the conventional statistical optimization scheme.

The combination parameter $\delta_s = Q_s/w_s$ in the normal equation (7.43) can completely separate the contributions of the observation system (covariance structure) from influences of observation quality w_s, so that the combination process (collaborative algorithm) is not affected by the observation errors. Therefore, it is conducive to the deep fusion of various geodetic variations from multiply monitoring systems with the diverse observation types, different spatial distribution and various observation system structure.